

Research Article

Paradigm Change of Pegmatite Formation – Where Does the Water Come From?

Rainer Thomas^{1*}, Gregor Brümmer² and Klaus Scheiblauber³¹Rainer Thomas, Im Waldwinkel 8, D-14662 Friesack, Germany²Gregor Brümmer, Montsanssaisir-Verlag, Auforsterstrasse 7a, D-84518 Alzheim, Germany³Klaus Scheiblauber Joh. NEMEZ& Co GmbH, Pernerstorferstrasse 29, A-2700 Wiener Neustadt, Austria

*Corresponding author: Rainer Thomas, ImWaldwinkel 8, D-14662 Friesack, Germany

Received: July 28, 2025; Accepted: July 31, 2025; Published: August 05, 2025

Abstract

We show in this contribution, mainly on the example of diamond and boron extracted from grey cast iron and natural samples from the Variscan mineralizations of the German and Czech Erzgebirge, that both disciplines, metallurgy and mineralogy, can together find a way to explain a surprising observation in nature. Of course, the interpretation of the natural observation of diamond and boron, found in the Earth's crust, is in the hands of the geologist. Nevertheless, a deeper understanding of thermodynamics guides any material scientist in explaining the existence of unexpected phases.

Keywords: Supercritical fluid, Grey cast iron, Diamond, First natural boron, Pegmatite formation

Introduction

Water has a fundamental meaning for the pegmatite formation. Niggli (1920) [1] has already explicitly discussed that. Yuan et al. (2021a and 2021b) [2,3] discuss a paradigm change, however, not based on the origin of water. Some authors ignore the extraordinary meaning of water [4]. Generally, it is accepted that the water for the pegmatites comes from the hosting granite. We will now show that this, at least for a lot of pegmatites, does not apply. Thomas (2023a) [5] and references in that) has shown in a row of contributions that supercritical fluid (SCF) or supercritical melts (SCM) have left their traces, especially in pegmatites and related mineralizations. A row of authors experimentally and theoretically studied the properties of such media. At this place we call Ni et al. (2017) [6], Ni (2023) [7], and Sun et al. (2023) [8]. Regarding the redox behavior, there is little information, mainly in the form of experimental speculations. Over the transition from the supercritical to the critical and under critical states, there is not much information. By doing exceptional work in a very different field (producing grey cast iron), new information and ideas could be obtained. The first surprising observation was the remarkable amount of diamond. A rough estimation gives a diamond volume of about 0.06%. That is more content than in kimberlite, the mother rock of diamonds. During the study of grey cast iron [9], we found, within the matrix, a lot of diamonds (spherical crystals from $< 0.3 \mu\text{m}$, over $1.5\text{--}2.0 \mu\text{m}$, and aggregates ≥ 10 to $20 \mu\text{m}$) – see Figure 1. In Figure 2, a typical Raman spectrum of such a cast iron-diamond is shown. Besides diamonds, we found after dissolution of the matrix many small ($1\text{--}2 \mu\text{m}$) spherical boron crystals (see Figure 3) that demonstrate at strong reducing conditions. In nature, particularly in the Earth's crust, such conditions are scarce. Therefore, Boron is not a mineral – it is missing in the mineral systems. However, borates are widespread minerals.

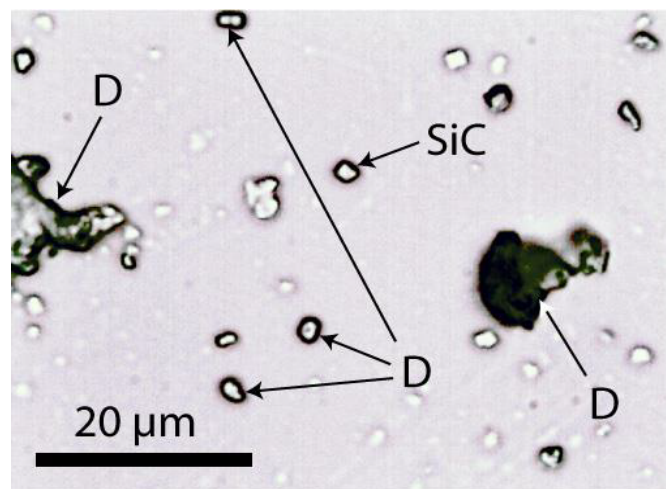


Figure 1: Diamonds (D) and silicon carbide (SiC) crystals after dissolving of grey cast iron in hydrochloric acid (25%) placed on a microscope slide.

In this contribution, we will now show that such strongly reducing conditions are not rare at the Variscan tin mineralizations of the Erzgebirge/Germany. The first hints are the omnipresent graphite crystals in many minerals (beryl, cassiterite, quartz, topaz, Zinnwaldite), which were overlooked in the past. Another essential hint was the wrongly interpreted occurrence of hydrogen in the fluid phase of melt inclusions in pegmatite quartz from Ehrenfriedersdorf [10]. With Raman spectroscopy, we determined $X_{\text{CO}_2} = 0.160 \pm 0.040$; $X_{\text{CH}_4} = 0.260 \pm 0.080$, and $X_{\text{H}_2} = 0.580 \pm 0.050$. Another proof came from a new fluid inclusion type in so-called hydrothermal-grown beryl, grown from supercritical fluid [5]. The vapor phase is entirely composed of methane.

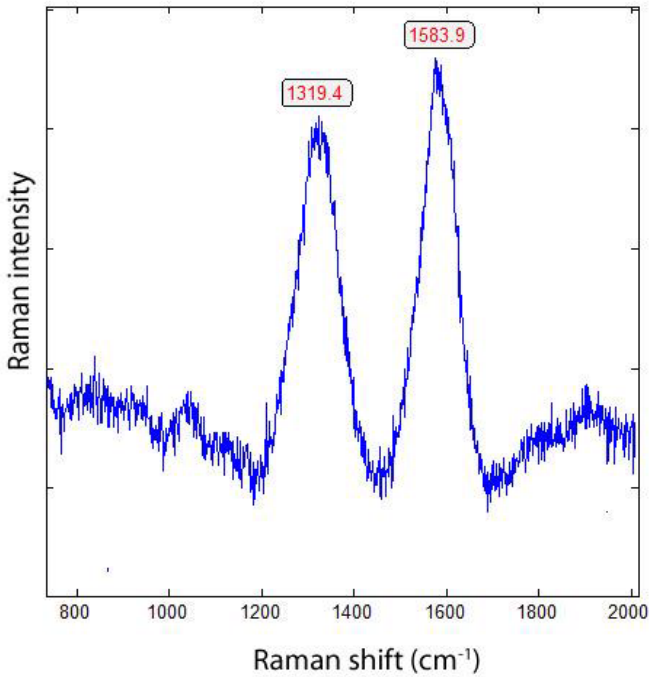


Figure 2: Raman spectrum of diamond spheres (Figure 1) dissolved (using hydrochloric acid) out of the grey cast iron.

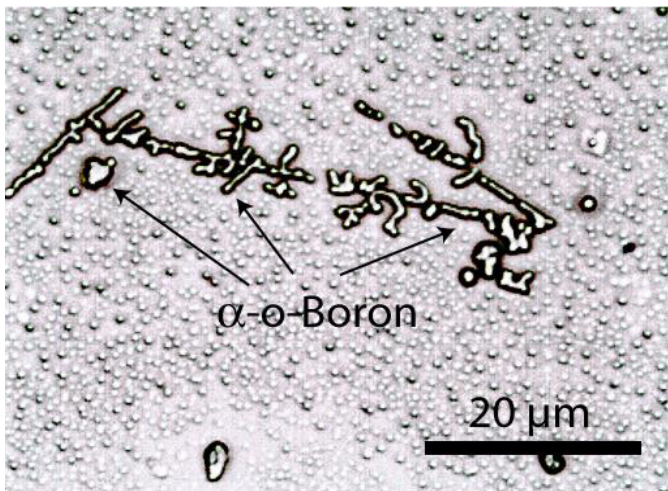


Figure 3a: Crystals, most of them spherical, of α -rhombohedral boron dissolved out of ductile cast iron and placed on a microscope slide. The spheres in the background are also boron, sometimes diamonds, and borcarbides.

As we see in Figure 2, there is a shift of the main Raman line from 1333.5 cm^{-1} to 1319.4 cm^{-1} . Because no ^{13}C -rich carbon is used, the shift is the result of the insertion of Si-Si [11]. Free silicon carbide (SiC) is a scarce component of the grey cast iron and of controversial origin; however, it is a minor component in the boron. Orthorhombic iron carbide (Fe_3C) has two broad bands at 1342 and 1580 cm^{-1} [12]. Orthorhombic (Pnma) cohenite (Fe_3C), as a natural analog, is tin-white and opaque metallic, and has only Raman bands in the low frequency range (RRUFF database, see Lafuente (2016) [13].

In addition to diamond, many small spherical crystals of α -rhombohedral boron are present. Besides the spherical boron crystals, they are also flat, rectangular plates. These plates are completely colorless, and the spherical crystals are too.

That diagram (Figure 3b) shows clearly that boron oxide would most probably not exist in a molten metal that contains C and Si, and certainly not in Mg-treated ductile iron. If nitrogen is dissolved in such a melt, boron nitride would appear only in the absence of Ti and Zr. As Mg-treatment removes nitrogen from a ductile iron melt, boron nitride would most likely not occur. Boron carbide is well known as a tool to improve the strength and hardness of certain steel qualities, and its existence is slightly preferred in comparison to iron carbide [14]. But Iron carbide is effectively avoided by reasonable Si levels above 1,5%. The sample discussed had a Si-content of 2,7% and was free of iron carbide. Thus, silicon avoids the appearance of $\text{Fe}_3(\text{C}, \text{B})$ -carbides as well as Fe_2B phases; consequently, the small amount of boron included ends up as separate boron- and boron carbide microphases within the matrix.

Table 1 shows the results of the α -boron extracted from grey cast iron. The colorless spheres of boron have a diameter of $2 \mu\text{m}$ (Table 1 and Figure 4).

E. Weintraub [17] first prepared pure elementary boron in 1909-1911 after a lot of misunderstanding. According to Oganov (2010)

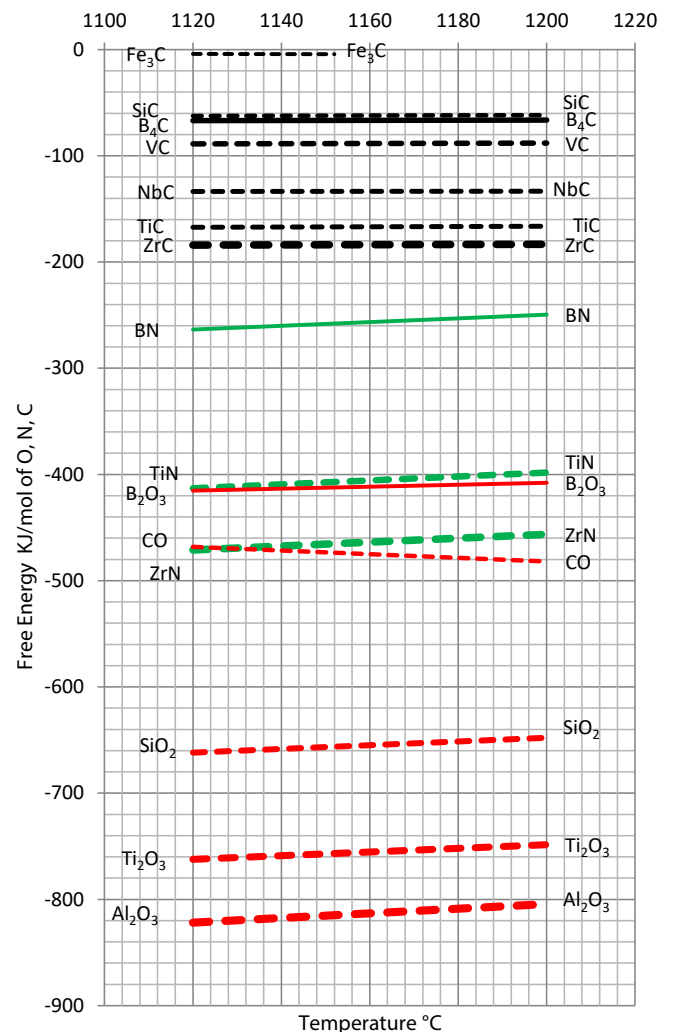


Figure 3b: A view on the free energy of various well-known metallurgy, oxides, nitrides, and carbides.

Table 1: Measured important Raman lines of α -boron extracted from ductile cast iron (Thomas et al., 2025) [9] using the Raman line 532 nm, (the modes are according to Werheit et al., 2010) [15].

| α -Boron | [cm ⁻¹] | Mode | n | Werheit et al. (2010) [cm ⁻¹] |
|-----------------|---------------------|-----------------|----|---|
| First order | 553.6 | | 3 | 552 |
| | 575.2 ± 1.50 | E _g | 14 | 589 |
| | 591 | E _g | 1 | 589 |
| | 771.5 | E _g | 1 | 778 |
| | 795.4 ± 1.99 | A _{1g} | 11 | 795 |
| | 938.6 | A _{1g} | 1 | 934 |
| | 1096.2 ± 5.35 | | 15 | 1094 |
| Second order | 1403.2 | | 5 | 1409 |
| | 1583.6 | | 3 | 1582 |
| | 1708.1 | | 3 | 1710 |

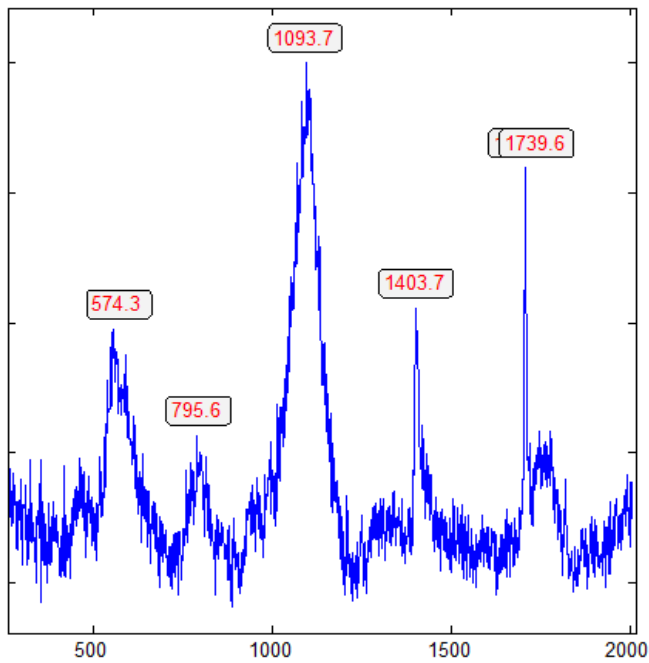


Figure 4: Raman spectrum of α -rhombohedral boron (from Figure 3), contaminated by β -rhombohedral boron and boron carbide, shown by the strong and broad Raman band (A_{1g} + E_g) at 1093.7 cm⁻¹, typical for the β -rhombohedral boron [15] and the main peak of boron carbide around 1100 cm⁻¹ [16].

[18], most of the discoveries related to pure boron were done in two “waves” – 1957–1965 and 2001–2009. Boron has been found in star dust and meteorites, but does not exist in the high-oxygen environment of the Earth. That is the state today. We will show that α - and β -Boron, together with boron carbides, can be found not only in meteorites but also in Earth’s material, which has significant importance and is the first observation ever. The rare appearance in different samples documents the strong reducing conditions of the supercritical fluid or melt (Figure 5).

Besides diamond and boron, there are a couple of minerals that demonstrate a connection between the Earth’s mantle and crust via supercritical fluid and/or melts. Because we find such minerals first and foremost in pegmatites and related mineralisations, we will summarize here the data.

Natural Occurrence of Boron in Pegmatites and Related Mineralization

Up to now, boron in nature is not present. Only a lot of boron complexes and straightforward compounds are well known (e.g., boric acid, tourmaline). To form boron, strong reducing conditions are necessary. Astonishing is the occurrence of boron as smooth spherical inclusions in some minerals (cassiterite, quartz, topaz, Zinnwaldite) of the Variscan Erzgebirge, similar to the boron in the ductile cast iron. Such spherical crystals occur in different minerals in Ehrenfriedersdorf, Sadisdorf, Zinnwald, here also in the mineral Zinnwaldite. Of course, the boron is mainly a mixture of boron, boron carbide, and other minor phases, making the identification very difficult. Also, the reverse case is possible: traces of boron in diamond from Zinnwald. In Figure 6, such an ellipsoid-shaped boron crystal in cassiterite (found in 2023) from Ehrenfriedersdorf (Sn-58) from

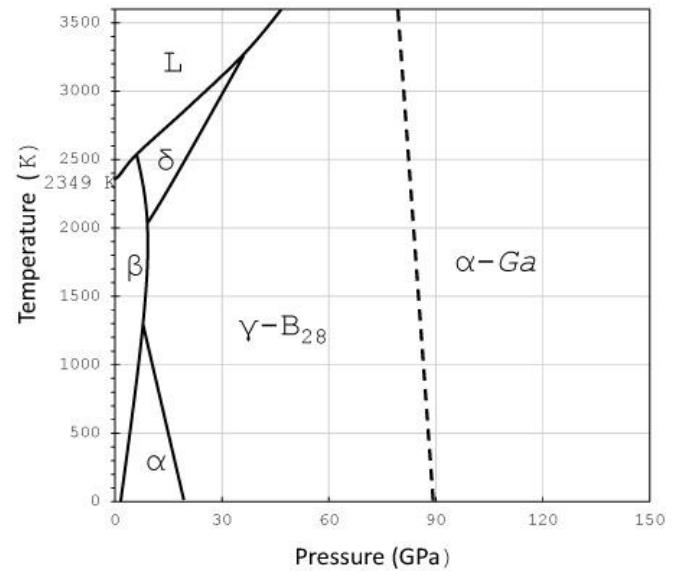


Figure 5: Schematic phase diagram of boron from Organov et al. (2009, 2010) [18-19]. The γ -B₂₈ and α -Ga types are special high-pressure phases, which are not crucial in our viewing and are not important here. α , β , and δ stand for α -, β -, δ -boron; and L for liquid or molten boron.

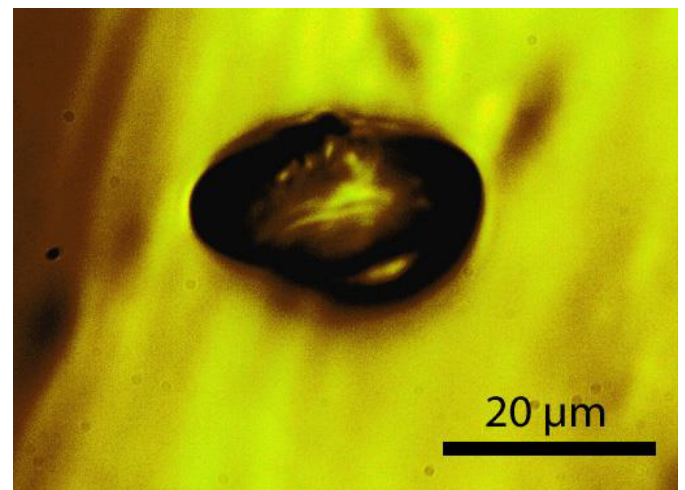


Figure 6: Spheroid of Boron in cassiterite from Ehrenfriedersdorf (Sample: Sn-58).

Magdalena vein, second gangway (Mining Academy Freiberg, No. 11814) is shown.

The Raman spectrum is depicted in Figure 7. The main line at 478 cm^{-1} corresponds to $A_{1g} + E_g$ of β -rhombohedral boron; also, the bands at 630 (A_{1g}) and 773 cm^{-1} . The median strong band at 1106 cm^{-1} is, according to Werheit et al. (2010) [15], from β -rhombohedral boron with about 0.11 at% carbon. The 1082 cm^{-1} Raman band, according to Roma et al. (2022) [16], is attributed to the boron carbide. The classification by the mixture of different B-phases according to Roma alone is not possible, especially since traces of boron carbides and β - Si_3N_4 can be present [20].

Besides the spherical shape, there are also black whisker-like crystals in α -quartz from Zinnwald present (Figure 8). If the crystals

are thin enough, the needles are transparent with a yellow shade. Often we observe beside boron diamonds. The largest diamond crystal, beside a large boron crystal, has a diameter of 20 μm . In the α -quartz crystal, there are zones with hundreds of diamond and boron whiskers (Figures 8 and 9).

The α -quartz crystal from Zinnwald contains a lot of whisker or needle-like α -boron crystals, which include constant small amounts of β -Boron. Particularly, the ends of those boron needles show a strong Raman band at 456 cm^{-1} ($A_{1g} + E_g$) characteristically for β -rhombohedral Boron [15]. In Table 2 are the measured Raman bands of natural α - and β -Boron summarized. Because the small needles are in quartz, the Raman measurements in the low-frequency range are difficult due to the strong quartz band (at 464 cm^{-1}). The tetragonal metastable δ - and ϵ -Boron was not found up to now (Table 2).

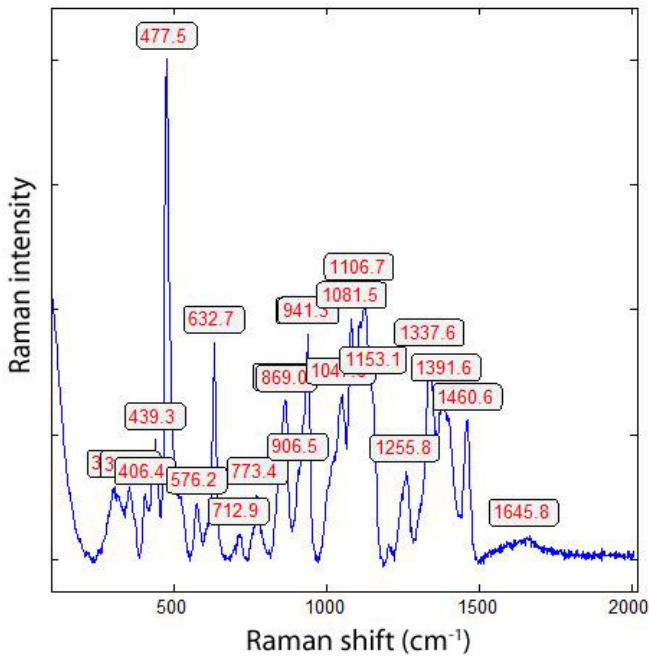


Figure 7: Raman spectrum of the boron crystal shown in Figure 6. The strong line 478 cm^{-1} is from the β -rhombohedral boron [15].

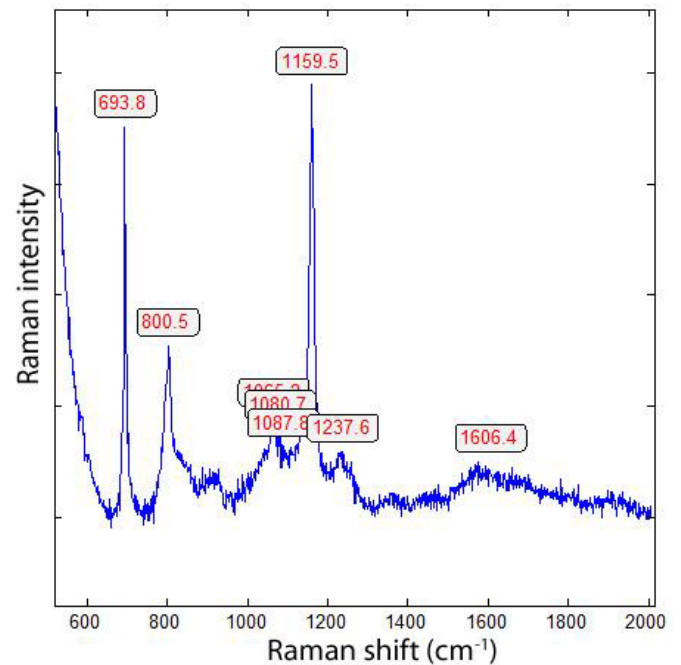


Figure 9: Raman spectrum of the boron needle in Figure 8. The bands at 694, 800, (1088), 1160, 2238 cm^{-1} are, according to Werheit et al. (2010) [15], typical for α -rhombohedral boron.

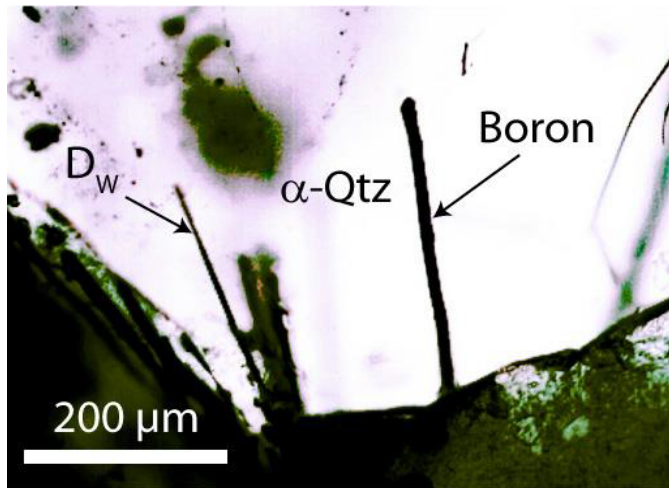


Figure 8: α -rhombohedral boron crystal needle in α -quartz from Zinnwald beside a diamond whisker (D_w). The black part in Figure 8 is a graphite aggregate, containing boron, indicated by a strong line at 781.4 cm^{-1} (in Werheit et al., 2010 [15] the 778 cm^{-1} line).

Table 2: Measured important Raman lines of α - and β -boron (532 nm laser), modes according to Werheit et al. (2010) [15].

| α -Boron | [cm^{-1}] | Mode | n | Werheit et al. (2010) [15] [cm^{-1}] |
|-----------------|----------------------|----------------|----|---|
| First order | 693.9 \pm 0.81 | A_{1g} | 11 | 694 |
| | 747.0 \pm 0.24 | | 5 | 750 |
| | 774.8 \pm 6.68 | E_g | 5 | 778 |
| | 799.8 \pm 1.05 | A_{1g} | 10 | 795 |
| | 870.9 \pm 2.63 | E_g | 10 | 873 |
| | 1159.4 \pm 0.90 | | 11 | 1160 |
| Second order | 1244.9 \pm 5.20 | | 7 | 1238 |
| | 1579.6 \pm 2.20 | | 10 | 1582 |
| β -Boron | | | | |
| First order | 219.0 | | 1 | 219 |
| | 282.0 | | 1 | 282 |
| | 305.0 \pm 1.65 | | 5 | 309 |
| | 459.9 \pm 2.62 | $A_{1g} + E_g$ | 6 | 456 |
| | 480.6 | | 1 | 480 |
| | 689.0 \pm 3.20 | | 5 | 685 |

Those remarks on boron should be enough to show the strong reducing conditions during the interaction of supercritical fluids with the Variscan mineralization. If we use the pressure-temperature diagram for SiO₂ polymorphs from Frondel (1962) [21] and use the results from Zinnwald quartz [22], the coexistence of α-quartz with coesite results in a more or less exact temperature value of 1300°C and a pressure of nearly 3,4 GPa. Such values are realistic for supercritical fluid if they meet the crustal granitic rocks. However, these values are too low according to the experimentally determined equilibrium curve for diamond-graphite [23] (Figure 10).

Proofs for the Deep Origin of Water as a Supercritical Fluid or Melt

In this chapter, we will summarize proofs found by the first author in recent years showing the influence of supercritical fluids or melts as carriers of high-pressure and high-temperature minerals. Or, in reverse, the high-pressure and high-temperature minerals, mostly spherical, in Variscan pegmatites, granite, and other mineralizations, demonstrate clearly that the input of supercritical fluids or melts has a significant influence on these mineralizations. That story is obvious. However, the formation of diamond and boron whiskers in quartz and moissanite whiskers in beryl crystals raises some questions: What is the mechanism of the formation of such whisker-like crystals far away

from the experimentally determined equilibrium conditions? Is the formation of such exceptional crystals the result of catalytic action? Which catalyst is working? Table 3 shows some mineral phases in minerals of deposits in the Variscan Erzgebirge/Germany. These are generally minerals formed at high pressures and high temperatures, and not at the place of mineralization. The whiskers of diamond, moissanite, and boron are obviously crystallized at the place of mineralization in the crustal region.

In this contribution, we have restricted ourselves to examples from the Variscan mineralisations in the German and Czech Erzgebirge. However, we know that in a lot of other pegmatites and granites, diamonds and similar HP and HT minerals are present: Königshain granite and his miarolitic pegmatites, as well as quartz veins in the Lusatian Mts, Bornhom pegmatites [29], Volyn pegmatites [26], pegmatites from the Reinbolt Hills/East Antarctica [25], and many others.

Discussion

Schröcke (1954) [30] has already demonstrated this with his excellent generalized sections of II. gangway of the Prinzler West cross-cut in the Sauberg mine near Ehrenfriedersdorf, where the granite's water alone cannot form the amount of pegmatite bodies and streaks. We need an extra source of water to bring together minerals (beryl-II, α- and β-boron, boron carbide, diamond, coesite, cristobalite X-I, graphite, silicon carbide, stishovite) as well as CH₄, H₂ and D₂ [5,10,31]. That means at least that the supercritical fluids and melts will feed a large amount of water coming from the mantle regions. The supercritical fluids/melt have a large amount of energy, which can, at the transition to the under critical stage, make the necessary room for pegmatites and vein mineralizations. That means at least a lot of observations in the past are of secondary meaning. At that place, the extreme element enrichment according to Lorentzian-like curves as proof of the meaning of supercritical fluids is foregone, because we have discussed this point enough [32]. Because elemental boron in an oxidized surrounding and high temperatures is not stable, it must form more stable compounds, like boric acid and many other B-bearing minerals. Another critical point is that a large part of boron comes directly from the mantle region.

Appendix: Microscopy, Raman Spectroscopy, and Extraction of Diamond and Boron from the Grey Cast Iron Sample No. 2

Besides a polarization microscope for transmission and reflection (JenaLab Pol), we performed all microscopic and Raman spectroscopic studies with a petrographic polarization microscope (BX 43) with

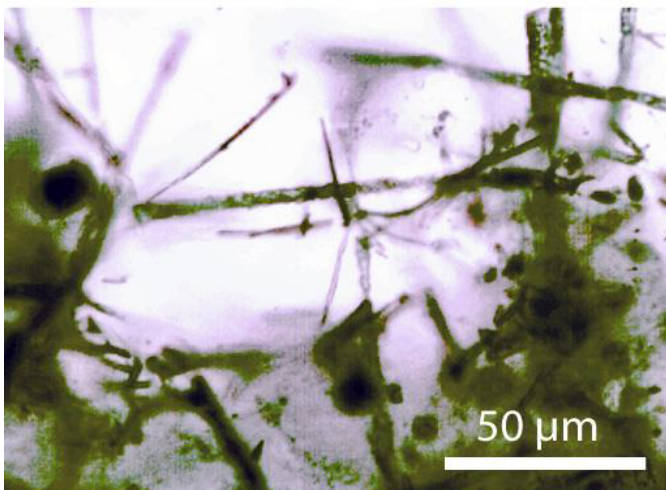


Figure 10: A mesh of diamond and boron whiskers in pegmatite quartz from Zinnwald. The black dot in the middle of the left side is also a diamond containing remnants of α- and β-boron [22].

Table 3: Mineral phases in pegmatites determined with Raman spectroscopy that demonstrate the foreign (deep) origin (selection from more cases).

| Mineral | Mineral host | Deposit | References |
|--------------------------|---|---|---|
| Diamond, Lonsdalite | Quartz, Topas, Fluorite, Cassiterite, Zinnwaldite | Ehrenfriedersdorf, Greifensteingranite, Annaberg granite, Sadisdorf, Zinnwald granite and pegmatite | Thomas (2025) – [20] and references in this. Thomas and Trinkler, 2024 [24], Thomas et al., 2023a [5] |
| Boron | Quartz | Zinnwald | This work |
| Moissanite | Beryl | Ehrenfriedersdorf | Thomas et al., 2023c [25] |
| Coesite | Quartz, Topaz, Prismantine | Ehrenfriedersdorf, Greifenstein granite, Waldheim | Thomas (2025) [22], Thomas et al., 2022a [26] |
| Orthorhombic cassiterite | Cassiterite | Ehrenfriedersdorf, Krupka, Schlaggenwald | Thomas (2023b) [27] |
| Cristobalite-X-I | Topaz | Greifenstein granite | Thomas et al., 2023 [28] |

a rotating stage coupled with the EnSpectr Raman spectrometer R532 (Enhanced Spectrometry, Inc., Mountain View, CA, USA) in reflection and transmission. The Raman spectra were recorded in the spectral range of 0–4000 cm^{-1} using an up-to-50 mW single-mode 532 nm laser, an entrance aperture of 20 μm , a holographic grating of 1800 g/mm, and a spectral resolution of 4 cm^{-1} . Generally, we used an objective lens with a magnification of 100x: the Olympus long-distance LMPLFLN100x objective (Olympus, Tokyo, Japan). The laser power on the sample is adjustable down to 0.02 mW. The Raman band positions were calibrated before and after each series of measurements using the Si band of a semiconductor-grade silicon single-crystal. The run-to-run repeatability of the line position (based on 20 measurements each) is $\pm 0.3 \text{ cm}^{-1}$ for Si ($520.4 \pm 0.3 \text{ cm}^{-1}$) and 0.4 cm^{-1} for diamond ($1332.7 \text{ cm}^{-1} \pm 0.4 \text{ cm}^{-1}$ over the range of 80–2000 cm^{-1}). The FWHM = $4.26 \pm 0.42 \text{ cm}^{-1}$. FWHM is the Full-Width at Half Maximum. We also used a water-clear natural diamond crystal (Mining Academy Freiberg: 2453/37 from Brazil) as a diamond reference (for more information, see Thomas et al., 2023) [28]. The zero-point position for the Raman spectroscopic measurements is checked before each measurement campaign. For the identification of mineral phase, we used Hurai et al. (2015), the RRUFF database by Lafuente et al. (2015) [13], and Liu et al. (2024) [12].

Extraction of Diamond and Boron from Grey Cast Iron

To the extraction of diamond and boron from the grey cast iron No. 2 [9], we have, from this sample (15.20 g), in two steps, 1.90 g and 1.60 g dissolved in hydrochloric acid (25%). The first solution was rejected for the removal of the diamond used for the preparation. The second fraction was cleaned with distilled water and concentrated in a trough washer of a petri dish. With a micropipette, a droplet with diamond and boron is placed on a microscope slide to dry. By skillfully placing many sub-micrometer-sized grains of diamond and boron, it was possible to determine the Raman spectra from such small things [33].

Acknowledgment

Many colleagues have provided relevant advice and documentation for the success of this work over the years.

References

- Niggli P (1920) Die leichtflüchtigen Bestandteile im Magma. *Teubner in Leipzig*. Pg: 272.
- Yuan Y, Moore LR, McAleer R, Yuan S, Ouyang H, et al. (2021a). A new paradigm for pegmatite formation: Generation of pegmatitic textures in a closed, isochoric system implied by the formation of miarolitic-class, segregation-type pegmatites in the Taishanmiaio batholith, China. *Goldschmidt* 2021.
- Yuan Y, Moore LR, McAleer R, Yuan S, Ouyang H, et al. (2021b) Formation of miarolitic-class, segregation-type pegmatites in the Taishanmiaio batholith, China: The role of pressure fluctuations and volatile exsolution during pegmatite formation in a closed, isochoric system. *American Mineralogist*. 106: 1559-1573.
- London D (2008) Pegmatites. The *Canadian Mineralogist*. Special Publication 10. 347.
- Thomas R (2023a) A new fluid inclusion type in hydrothermal-grown beryl. *Geology, Earth and Marine Sciences*. 5: 1-3.
- Ni H, Zhang L, Xiong X, Mao Z, Wang J (2017) Supercritical fluids at subduction zones: Evidence, formation condition, and physicochemical properties. *Earth-Science Reviews*. 167: 62-71.
- Ni H (2023) Introduction to advances in the study of supercritical geofluids. *Science China: Earth Science*. 66: 2391-2394.
- Sun Y, Liu X, Lu X (2021) Structures and transport properties of supercritical $\text{SiO}_2\text{-H}_2\text{O}$ and $\text{NaAlSi}_3\text{O}_8\text{-H}_2\text{O}$ fluids. *American Mineralogist*. 108: 1871-1880.
- Thomas R, Brümmer G, Scheiblaue K (2025) Unexpected carbon phases in grey cast iron – diamond, calcite, and methane. *Geology, Earth and Marine Sciences*. 7(4): 1-6.
- Thomas R, Webster JD (2000) Strong tin enrichment in a pegmatite-forming melt. *Mineralium Deposita*. 35: 570-582.
- Zaitsev AM (2001) Optical Properties of Diamond. A Data Handbook. *Springer*. 1-XI and 1-502 pages.
- Liu Q, Miao H, Liu W, Bu L, Yao J, Chen J, Wu F, Li L, Jing W (2024) Selective transformation of cementite: Graphitization or spheroidization. *Materials Today*. 61: 234-246.
- Lafuente B, Downs RT, Yang H, Stone N (2016) The power of database: The RRUFF project. In: Highlights in Mineralogical Crystallography, Armbruster T, Danisi RM (Eds: De Gruyter: Berlin, München, Boston 1-30.
- Bauer W (2009) Die Auswirkung kleiner Borgehalte auf die Ferrit-/Perlitbildung im Gusseisen. *Giesserei* 96: 22-31, more detailed in ÖGI-Projekt A. No. 46371: Die Rolle der Spurenelemente Bor, Phosphor und Stickstoff bei der Ferrit/Perlitbildung von Gusseisen mit Kugelgraphit. Austrian Foundry Institute, Leoben, Pg: 71.
- Werheit H, Filipov V, Kuhlmann U, Schwarz U, Armbrüster M, Leithe-Jasper A, Tanaka T, Higashi I, Lundström T, Gurin VN, Korsukova MM (2010) Raman effect in icosahedral boron-rich solids. *Science and Technology of Advanced Materials*. 11.
- Roma G, Gilles K, Jay A, Vast N, Gutierrez G (2021) Understanding first order Raman spectra of boron carbides across the whole stoichiometry range. *Physical Review Materials*. 5: 1-31.
- Weintraub E (1911). On the properties and preparation of the element boron. *J. Ind. Eng. Chem*. 3: 299-301.
- Oganov AR (2010) Boron under pressure: Phase diagram and novel high-pressure phase. NATO Science for Peace and Security Series B: Physics and Biophysics – Boron rich solids. Eds: By Orlovskaya N and Lugovy M. *Springer*. Pg: 207-225.
- Oganov AR, Chen J, Gatti C, Ma Y-M, Yu T, Liu Z, Glass CW, Ma Y-Z, Kurakevych OO, Solozhenko VL (2009). Press release Ionic high-pressure form of elemental boron. *Nature* 457: 863-867.
- Werninghaus T (1997) MicroRaman spectroscopy investigations of hard coatings. Dissertation, TU Chemnitz-Zwickau. Pg: 163.
- Frondel C (1962) The System of Mineralogy. Volume III, Silicate Minerals. John Wiley and Sons, INC. Pg: 334.
- Thomas R (2025) Diamond, diamond whisker, graphite, carbon, and coesite in a quartz crystal from Zinnwald, E-Erzgebirge. *Geology, Earth and Marine Sciences*. 7v: 1-6.
- Day HW (2012) A revised diamond-graphite transition curve. *Am. Mineralogist*. 97: 52-62.
- Thomas R, Trinkler M (2024) Monocrystalline lonsdaleite in REE-rich fluorite from Sadisdorf and Zinnwald/E-Erzgebirge, Germany. *Geology, Earth and Marine Sciences*. 6: 1-5.
- Thomas R (2023c) Diamond in pegmatitic sillimanite from Reinbolt Hills/East Antarctica. *Geology, Earth and Marine Sciences*. 5: 1-3.
- Thomas R, Davidson P, Rericha A, Recknagel U (2022a) Water-rich coesite in prismatine-granulite from Waldheim/Saxony. *Veröffentlichungen Museum für Naturkunde Chemnitz*. 45: 67-80.
- Thomas R (2023b) Unusual cassiterite mineralization, related to the Variscan tin-mineralization of the Ehrenfriedersdorf deposit, Germany. *Aspects in Mining & Mineral Science*. 11: 1233-1236.
- Thomas R, Davidson P, Rericha A, Recknagel U (2023) Ultrahigh-pressure mineral inclusions in a crustal granite: Evidence for a novel transcrustal transport mechanism. *Geosciences*. 13: 1-13.
- Thomas R (2024) ^{13}C -rich diamond in a pegmatite from Rønne, Bornholm Island: Proofs for the interaction between mantle and crust. *Geology, Earth and Marine Sciences*. 6: 1-3.

30. Schröcke H (1954) Zur Paragenese erzgebirgischer Zinnlagerstätten. *Neues Jb. Mineral. Abh.* 87: 1-109.
31. Thomas R, Davidson P, Rericha A, Voznyak DK (2022b) Water-rich melt inclusions as “frozen” samples of the supercritical state in granites and pegmatites reveal extreme element enrichment resulting under non-equilibrium conditions. *Mineralogical journal (Ukraine)*. 44: 3-15.
32. Thomas R, Rericha A (2024) Extreme element enrichment, according to the Lorentzian distribution at the transition of supercritical to critical and under-critical melt or fluids. *Geology, Earth and Marine Sciences*. 6: 1-6.
33. Parakhonskiy G (2012) Synthesis and investigation of boron phases at high pressure and temperatures. Dissertation at the University of Bayreuth. Pg: 117.

Citation:

Thomas R, Brümmer G, Scheiblaue K (2025) Paradigm Change of Pegmatite Formation – Where Does the Water Come From? *Geol Earth Mar Sci* Volume 7(5): 1-7.